ELSEVIER

Thin Solid Films 342 (1999) 214–220

thin solid films

# Thin film TiC/TaC thermocouples

Hemanshu D. Bhatt[a], Ramakrishna Vedula[a,*], Seshu B. Desu[a], Gustave C. Fralick[b]

[a]*Materials Science and Engineering Department, 213 Holden Hall, Virginia Tech, Blacksburg VA 24061, USA*
[b]*NASA Lewis Research Center, 21000 Brookpark Road, Cleveland OH 44135, USA*

Received 2 February 1998; accepted 5 June 1998

**Abstract**

TiC and TaC thin films were investigated, for the first time, for thin film thermocouple applications. Thin films of TaC and TiC were deposited on electronic grade alumina substrates using the r.f. sputter deposition technique. Sheet resistance of the thin films was measured using a four point probe. It was observed that the sheet resistance of the films depends critically on the deposition parameters such as substrate temperature during deposition, sputter gas pressure and r.f. power used. The deposition parameters were optimized to yield the lowest sheet resistance of the thin films at room temperature. The thermoemf of the deposited films was measured as a function of temperature in a vacuum using a home made device. It was observed that thin films of TaC and TiC yield fairly high and stable thermoemf throug hout the temperature range of stability. Under the optimized deposition conditions, thin film thermocouples were fabricated. The thermocouples were calibrated against temperature and the output was measured in vacuum (pressure $< 10^{-6}$ Torr). TiC/TaC thermocouples yield stable output up to 1350 K, temperatures above which breakdown occurs. The thermocouple output was theoretically estimated from the thermoemf measured, and compared. It was observed that these thermocouples yield reproducible output in the temperature range of stability and hold excellent potential for high temperature thin film temperature sensor applications in vacuum or inert atmospheres. 

*Keywords:* Thin film thermocouples; Seebeck coefficient; Carbides; Titanium carbide

## 1. Introduction

Thermoelectric thin films have been used for several micro sensor applications which include heat flux sensors [1], strain gages [2], radiation sensors [3], pressure sensors [4], electrical power sensors [5], thin film thermocouples [6–8] and flow sensors [9]. This is essentially because, thin films offer numerous advantages over conventional bulk sensors such as excellent spatial resolution, fast response and minimal disturbance to the component being monitored [10,11]. In addition, CMOS processes could be applied in the fabrication of thin film sensors, which substantially reduces the cost of production [12]. In the case of temperature measurement systems, thin film thermocouples [13] and resistance thermometers [14] have been studied extensively.

Conventionally, platinumplatinum–10% rhodium thermocouples have been used for thin film thermocouple applications. However, recent studies have suggested, PtPt–Rh thermocouples present some problems at temperatures around 800–900°C such as substrate reaction, coalescing of films due to electromigration forming islets disturbing the electrical continuity of the films, rhodium oxidation resulting in inconsistencies in the thermocouple output, poor adhesion and so on [15,16]. Consequently, several materials have been investigated for thin film thermocouple applications. These include, indium tin oxide (ITO), antimony tin oxide (ATO), fluorine doped tin oxide [17], silicides of molybdenum, tantalum, rhenium, titanium and tungsten [18], ruthenium oxide, iridium oxide [19], lanthanum strontium cobalt oxide [20] etc.

High temperature thin film thermocouples present additional difficulties primarily because of smaller diffusion distances ($\sim$1 μm) compared with wire thermocouples ($>$500 μm). Hence, the primary criteria for selecting candidate materials are high melting point, stability of phase, chemical composition and microstructure in the thin film form, fairly large and stable electrical conductivity and Seebeck coefficients throughout the temperature range of operation, and easy and straight forward thin film fabrication process. Moreover, in applications involving oxidizing environments, the resistance of the candidate materials to oxidation also plays an important role.

In this study, titanium and tantalum carbide thin films

* Corresponding author. Tel.:+001 540 231 5994; fax:+001 540 231 8919.
*E-mail address:* vramakri@vt.edu (R. Vedula)

0040-6090/99/$ - see front matter 
PII: S0040-6090(98)00963-8

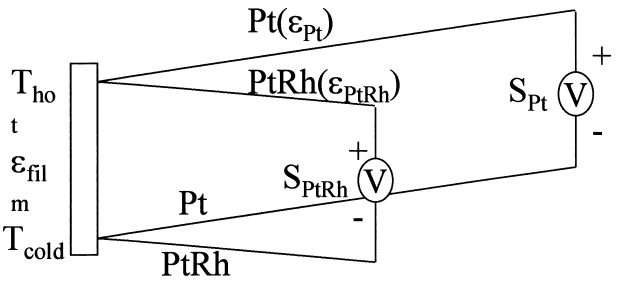


Fig. 1. Principle of measurement of Seebeck coefficient of TiC and TaC thin films.

were investigated, for the first time, for high temperature thin film thermocouple applications in inert or vacuum environments. Earlier, transition metal carbides were studied extensively as interesting engineering materials, (e.g. as cermets in the hard metals industry) owing to their extremely high melting points, strength and good corrosion resistance [21]. Among many transition metal carbides, titanium carbide based composites particularly are used as cutting tools, plasma and flame spraying processes in air, etc. [22]. Tantalum carbide on the other hand also has extremely high melting point (3983°C, one of the highest known) as well as high mechanical hardness [23]. Its electronic and optical similarities with group IV nitrides (such as TiN) are also of interest [24]. However, the range of applications of the transition metal carbides is limited due to their poor oxidation resistance. There are several reports of physical vapor deposition (PVD) of these carbides in literature and the deposition of TiC and TaC is easy and straightforward. All these properties of TiC and TaC have prompted the present investigation for high temperature thin film thermocouple applications in vacuum or inert environments.

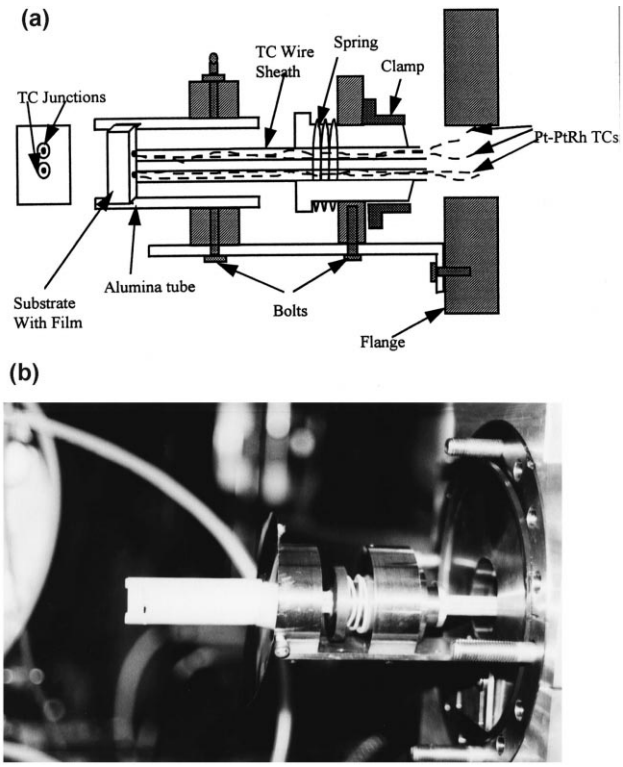


Fig. 2. Experimental setup for the measurement of thermoelectric properties of thin films (a) schematic, (b) photograph.

## 2. Experimental procedure

### 2.1. Thin film deposition and characterization

Thin films of TiC and TaC were deposited using r.f sputtering technique in a Denton Vacuum sputtering system. Sheet resistance of the deposited thin films was measured using a four point probe. The deposition conditions were varied to obtain the optimum sheet resistance of the thin films as well as substantial deposition rates. The r.f. power during deposition was varied from 50 to 100 W. A TiC (99.5% pure) target, 2 inches in diameter, 0.125 inches thick and a TaC target with identical specifications were used for deposition. The base pressure in the chamber was maintained between 3 and $10 \times 10^{-7}$ Torr. Argon was used as the sputter gas, and the deposition pressure was varied from 2 to 30 mTorr. Electronic grade alumina was used as substrate and the substrate temperature during deposition was varied from room temperature to 850°C.

Thickness of the deposited films was measured using Dektak profilometer and weight measurements. X-ray diffraction technique was used to study the phase development in the films. A Scintag diffractometer was used to record the XRD patterns using Cu $K_\alpha$ radiation. Chemical composition of the films was studied using electron spectroscopy for chemical analysis (ESCA) technique. Auger electron spectroscopy was used to study the interface characteristics and oxidation mechanism of the carbide thin films after exposure to high temperatures.

### 2.2. Thin film thermoelectric properties measurement

Thin films of TiC and TaC were deposited on alumina substrates using the optimized deposition conditions in the same sputtering system. From the deposited samples, resistors of width 4–4.5 mm were cut. These resistors were pasted on electronic grade alumina samples. The height of the samples was about 12 mm. The principle of measurement of Seebeck coefficient is shown in Fig. 1. Platinum and platinum–10% rhodium thermocouples were used to measure the thermoemf of the film. Each thermocouple was inserted in an alumina tube having two isolated holes for the two thermocouple legs. The two thermocouples were placed one on top of the other at a distance of 8 mm from each other. They were sealed using high temperature alumina cement. This was fixed to a stainless steel holder which could be slid lengthwise. The whole system was spring loaded to ensure contact with the resistor. Fig. 2 shows the experimental setup for high temperature thin

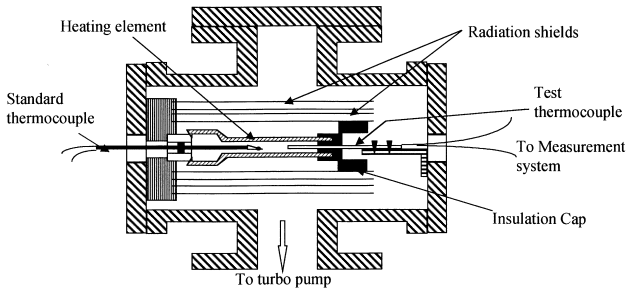


Fig. 3. Schematic of the test chamber for the calibration of the test thermocouples.

film thermoelectric properties measurement system. The top thermocouple was insulated during Seebeck coefficient measurement using molybdenum radiation shield to incorporate a temperature difference of about 15°C. The detailed description of the apparatus with the dimensions and performance analysis is given elsewhere [25]. The voltages generated between the Pt and Pt–Rh legs of the thermocouple and the temperatures of the hot and cold junctions were measured using a Tempbook 7-channel thermocouple readout system. The whole system was inserted in a high vacuum furnace, which has a built in temperature controller system and also maintains pressures less than $5 \times 10^{-7}$ Torr. From the data collected, Seebeck coefficients were plotted as a function of temperature. The equations used to evaluate the Seebeck coefficient are listed below. $S_{Pt}$ and $S_{PtRh}$ correspond to the voltage drops in the Pt and Pt–Rh legs of the two thermocouples respectively, $\varepsilon_{film}$, $\varepsilon_{Pt}$ and $\varepsilon_{PtRh}$ are the Seebeck coefficients of the film, Pt and Pt–Rh respectively and $T_h$ and $T_c$ are the temperatures of the hot and cold junctions, respectively.

$$S_{Pt} = -\varepsilon_{Pt}(T_h - T_c) + \varepsilon_{film}(T_h - T_c)$$

$$S_{PtRh} = \varepsilon_{PtRh}(T_h - T_c) + \varepsilon_{film}(T_h - T_c)$$

$$\varepsilon_{film} = \frac{S_{Pt}}{(T_h - T_c)} + \varepsilon_{Pt} = \frac{S_{PtRh}}{(T_h - T_c)} + \varepsilon_{film}$$

$$\Delta T_{theoretical} = (T_h - T_c) = \frac{S_{Pt} - S_{PtRh}}{\varepsilon_{PtRh} - \varepsilon_{Pt}}$$

### 2.3. Thin film thermocouple calibration and testing

Test thermocouples were deposited on alumina substrates using the optimized deposition conditions in the same sputtering system. Each leg of the thermocouples was deposited separately, and it was found that upon annealing, there is very good electrical continuity in the thermocouples. These thermocouples were calibrated using standard Pt/Pt–Rh thermocouples. Fig. 3 shows a schematic of the test chamber. The furnace was heated using boron nitride heating element by radiation. The test specimen was surrounded by several layers of molybdenum foil to prevent heating of the exterior of the chamber. Similar foil as well as a thick alumina disc were used as insulation caps to prevent the cold junctions of the test thermocouples from getting heated to high temperatures. Added to that, the cold junctions of the test thermocouples were fastened on to a stainless steel block, which was maintained at close to room temperature using circulated cooling water. The chamber was maintained at extremely low base pressures using a cryo pump. Fig. 4 shows the schematic view of a typical TiC/TaC test thermocouple. S-type platinum/platinum–10% rhodium wire thermocouples were used to determine the temperatures of the two cold junctions and the hot junction of the test thermocouples. The thermocouple output was measured using a Tempbook 7-channel thermocouple readout system. The thin film thermocouple output was measured between the two cold junctions as shown in Fig.4.

## 3. Results and discussion

### 3.1. Sheet resistance of the deposited films

The sheet resistance of the deposited films was measured using a four point probe technique. All the thin films studied in this section henceforth are 3000 Å thick as measured using weight measurements and Dektak profilometer. First, the deposition rate was measured for each of the deposition conditions and the thickness of all the films was maintained at 3000 Å.

#### 3.1.1. Dependence on r.f. power

Fig. 5 shows the variation of sheet resistance of the TiC and TaC thin films with r.f. power. With increasing r.f power of deposition, the sheet resistance decreases until 100 W beyond which there is little dependence. This effect could be attributed to the difference in the sputter yields of titanium, tantalum and carbon. From literature, it can be found that the sputter yields decrease in the order tantalum, titanium and carbon [26]. The effect of r.f. power of deposition on the sputter yields is more dominant at lower r.f. powers, whereas at higher r.f powers, there is smaller difference in the sputter yields. Accordingly, at lower r.f. powers, the deposition rate of tantalum is higher than that of titanium which in turn is higher than that of carbon. At higher r.f. powers, there is little difference in the relative deposition

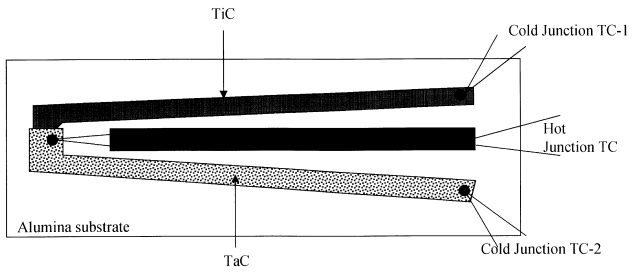


Fig. 4. A typical test thermocouple fabricated from TiC and TaC.

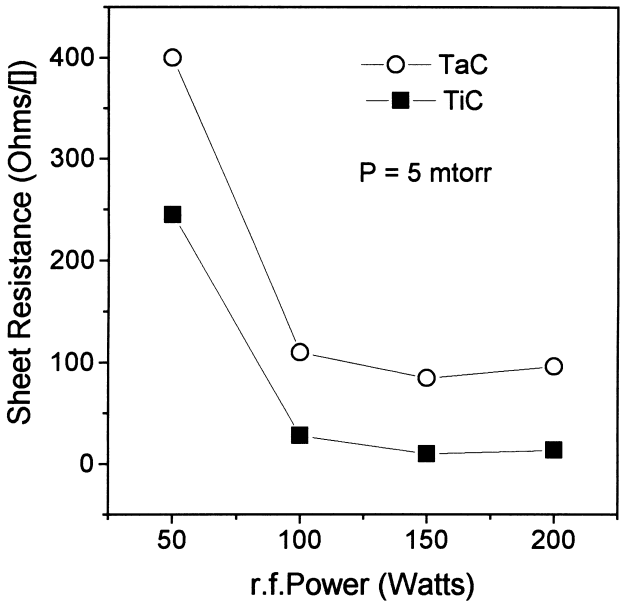


Fig. 5. Dependence of sheet resistance of TiC and TaC on r.f. power of deposition.

rates. Therefore, at lower r.f. powers, it is reasonable to expect that TaC is more deficient in carbon when compared to TiC (the difference in carbon content is close to 5%). Earlier reports on the dependence of electrical resistivity of TiC and TaC indicate that as the carbon deficiency in TaC and TiC increases, the electrical resistivity increases [27]. In our experiments, we observe that at higher r.f. powers, the sheet resistance is much lower compared to that at lower r.f. powers, which follows the above discussion. Also, this effect is more evident in the case of TaC when compared to TiC. There was no significant difference in the porosity of the films and hence such effects are neglected. From these experiments, it was found that 100 W was the optimum r.f. power taking into account, the limitations of the equipment.

### 3.1.2. Effect of sputter gas pressure

Fig. 6 shows the variation of sheet resistance of TiC as well as TaC thin films with sputter gas pressure during deposition. Both TiC as well as TaC show a marked increase in the sheet resistance with increase in the sputter gas. This effect could also be explained on the basis of differences in sputter yields of tantalum, titanium and carbon. At higher sputter gas pressures during deposition, there is a larger difference in the deposition rates of tantalum, titanium and carbon resulting in greater deviation in the stoichiometry which in turn increases the sheet resistance considerably. Also, there was oxygen incorporation into the films at higher pressures of deposition as indicated from composition analyses as well as depth profile analyses arising possibly due to the limitations of the equipment. The presence of oxygen in the films could also result in the increase in the sheet resistance of the films. From these results, it can be seen that lower pressures of sputter gas (argon) result in lower electrical resistivities.

### 3.1.3. Effect of substrate temperature

Fig. 7 shows the influence of the substrate temperature during deposition on the sheet resistance of TiC and TaC thin films. In the case of both TaC as well as TiC thin films there was no observable difference in the X-ray diffraction patterns of the films. Both the films were amorphous indicating no significant structural changes in the films. In the

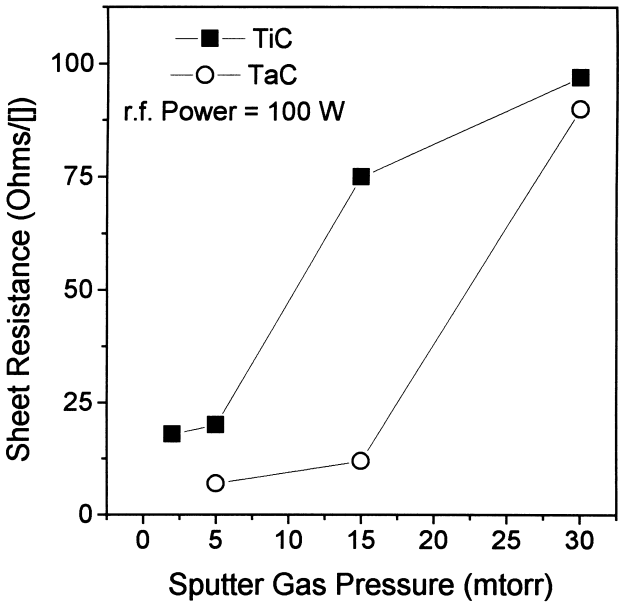


Fig. 6. Variation of sheet resistance of TiC and TaC thin films on the sputter gas (argon) pressure.

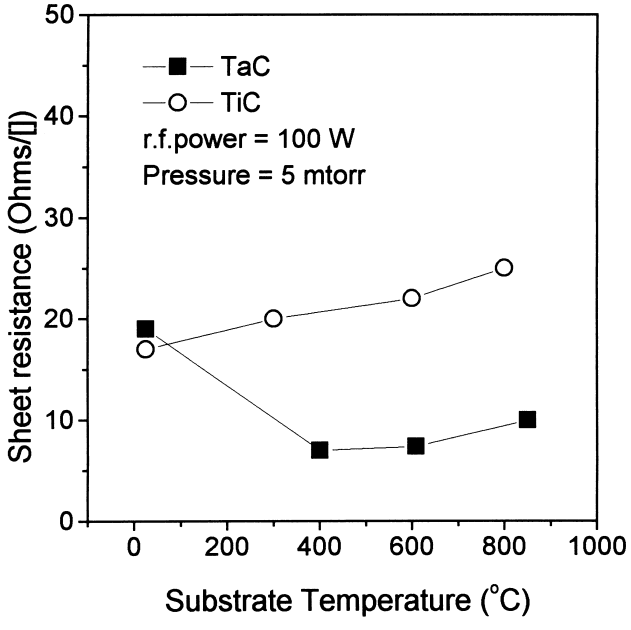


Fig. 7. Influence of substrate temperature during deposition on the sheet resistance of TaC and TiC thin films.

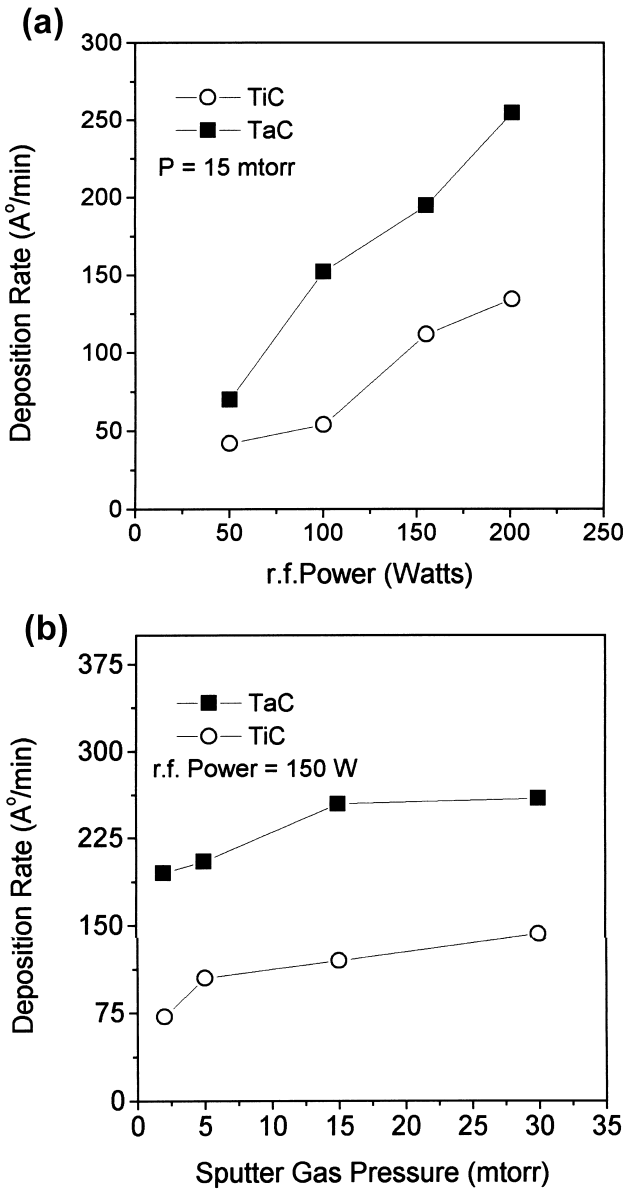


Fig. 8. Deposition rate dependence on (a) r.f. power of deposition, (b) sputter gas pressure.

case of TaC, the sheet resistance decreases sharply when the substrate temperature is increased from room temperature to 400°C. Further increase in the substrate temperature results in a slight increase in the sheet resistance. This trend can be explained on the basis of two effects viz., densification or grain growth and oxidation of the surface layers of the films. The former results in a decrease in the thin film resistivity while the latter results in an increase in the resistivity. Although a base pressure less than $5 \times 10^{-6}$ Torr is maintained before the argon gas is input into the chamber, there is a possibility of formation of a monolayer of oxide on the top of the carbide films which could result in an increase in the resistivity. However, it can be seen that, the increase in resistivity of the films is extremely small. These results indicate that a temperature of about 400°C is optimum for the deposition of carbide thin films.

### *3.2. Influence of sputter parameters on the deposition rates of TiC and TaC thin films*

The influence of r.f. power on the rate of thin film deposition is plotted in Fig. 8a while Fig. 8b shows the corresponding effect of sputter gas pressure. Both figures illustrate that at a constant sputter gas (argon) pressure of 15 mTorr, the higher the r.f. power or sputter gas pressure during deposition, the higher is the deposition rate. This is expected because as the r.f. power is increased, the number of particles striking the surface of the target is increased, resulting in a greater number of species released from the target. Consequently, the deposition rate is increased. This effect is observed both in TaC as well as TiC thin films. At a constant r.f. power of 150 W, it was observed that increasing the sputter gas pressure increases the deposition rate of the thin films. This can be attributed to the fact that, as the sputter gas pressure in the chamber increases the ion density in the plasma increases, resulting in greater deposition rates. Similar effects have been observed by several researchers and reported in literature [26].

From all these results it was found that the optimum deposition conditions to obtain substantial deposition rates and at the same time low sheet resistance were, r.f. power of 150 W, substrate temperature of 400°C and argon pressure of 2 mTorr during deposition. The thickness of the films was measured using a Dektak profilometer and was found to be about 3000 Å. All the results reported hereafter would be on thin films of TaC and TiC on alumina substrates deposited under the optimized sputter conditions. The fabrication of thin film thermocouples was also done using these parameters.

### *3.3. Thermoemf data of TaC and TiC thin films*

Thermoemf of TaC as well as TiC thin films was measured using the thin film thermoelectric properties measurement system shown in Fig. 2. Fig. 9 shows the thermoemf as a function of the absolute temperature for TiC and TaC thin films. During the measurement of the thermoemf of the films, it was not possible to control the temperature difference between the hot and cold junctions of the films accurately. This temperature difference varied between 10 and 40°C (a difference of 10–15°C is conventionally used for thermoemf measurements) and accounts for the large amount of scatter in the data presented. The trend however, appears to be similar to that reported earlier in literature [28]. From the thermoemf data in the thin film form, the thermocouple output of TiC/TaC thermocouples was estimated using a simple linear model. Test thermocouples were fabricated on alumina substrates and calibrated.

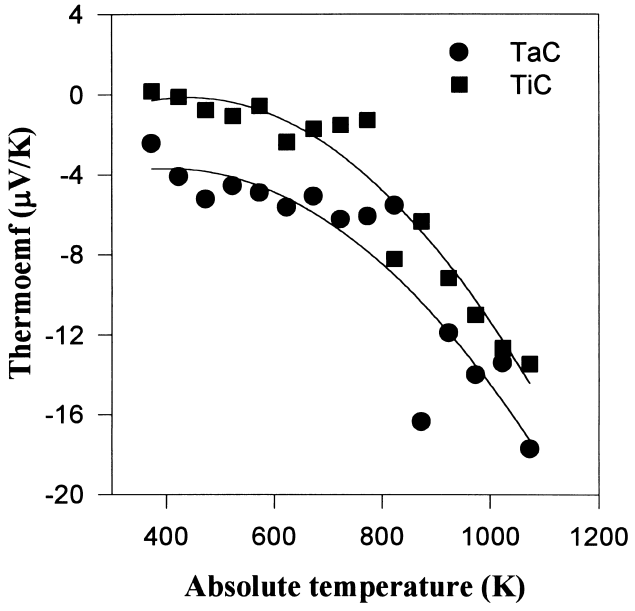


Fig. 9. Thermoemf of TaC and TiC thin films measured in vacuum (pressures $< 10 - 7$ Torr) as a function of temperature.

### *3.4. Thin film TiC/TaC test thermocouple calibration and performance*

Fig. 10 shows the performance of two thin film TiC/TaC thermocouples as a function of temperature in vacuum (pressure less than $5 \times 10^{-7}$ Torr). Also shown in the figure is the estimated output of the thermocouple calculated from the thermoemf of TiC and TaC thin films measured separately. From the figure, it is clear that there is very little difference in the thermocouple output of the two thermocouples testifying the consistency of the fabrication and the reproducibility of the data. The difference between the estimated and the experimentally determined values of the thermocouples could be attributed to the inaccuracies in the calculations arising possibly due to lack of control over the temperature difference between the hot and cold junctions of the thin films during thermoemf measurements. The second thermocouple was subjected to a temperature higher than the first (>1350 K) and this resulted in the breakdown of the thermocouple. From this observation, the temperature limit of operation of TiC/TaC thermocouples was determined to be about 1350 K.

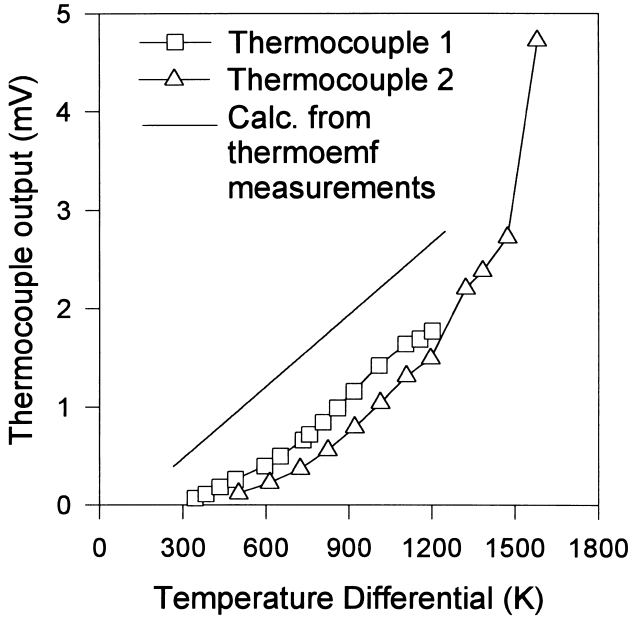


Fig. 10. Thermocouple output of two TiC/TaC thermocouples as a function of temperature.

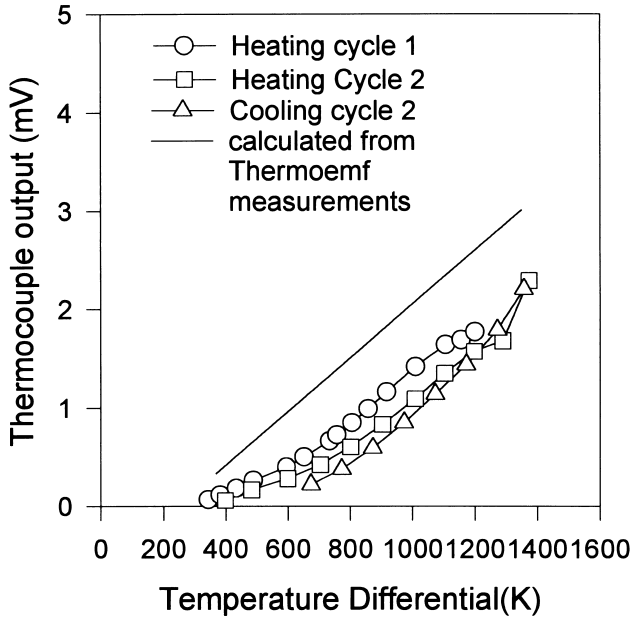


Fig. 11. Thermocouple output of TiC/TaC thermocouples as a function of temperature measured after several cycles of heating and cooling.

Fig. 11 illustrates the thermocouple output of thin film TaC/TaC thermocouples tested under several repeated cycles of heating and subsequent cooling. It can be observed that there is no significant change in the output of the test thermocouples during heating and cooling indicating stability of chemical composition, phase and thermoelectric properties of the films. The minor changes in the thermocouple outputs between heating and cooling cycles of operation could be attributed to any grain growth or densification of the films. The thermocouple, which was subjected to temperatures beyond the maximum temperature of operation, developed electrical discontinuities, which could be seen clearly with naked eye.

## 4. Conclusions

Thin films of TaC and TiC were deposited on electronic grade alumina substrates using r.f. sputtering technique. The sheet resistance of the deposited thin films was measured using a four point probe. It was observed that the electrical

properties of the thin films both TiC as well as TaC depend critically on the sputter deposition conditions and therefore, the deposition parameters were optimized to obtain the lowest sheet resistance of the thin films. TiC and TaC thin films were deposited under these conditions and thermoemf was measured using a home made device. The thermoemf of TiC and TaC thin films decreases as the temperature is increased. The output of TiC/TaC thermocouples was estimated based on the individual thermoemf data on thin films. Thin film thermocouples were successfully fabricated on alumina and calibrated against standard platinum/platinum–rhodium thermocouples. Thermocouple output was recorded as a function of temperature and the maximum temperature of stability of thermocouples was determined to be 1350 K. No significant change was observed in the output of the test thermocouples when they were subjected to several repeated cycles of heating and cooling indicating thermal and electrical stability of the thermocouples. The reproducibility of the thermocouple data was also tested and found to be satisfactory. It can be concluded that thin film TiC/TaC thermocouples hold excellent potential in high temperature thin film thermocouple applications in vacuum or inert atmospheres.

## References

[1] A. W. Van Herwaarden, P. M. Sarro, Sensors Actuat. 10 (1986) 321.
[2] J.F. Lei, H. Okimura, J.O. Brittain, Mater. Sci. Eng. A 111 (1989) 145.
[3] C. Shibata, C. Kimura, K. Mikami, Digest, First Sensor Symposium, IEE Japan, 1981, p. 221.
[4] F. Volklein, W. Schnelle, Sensors Mater. 3 (1991) 41.
[5] M. Klonz, T. Weimann, IEEE Trans. Instrum. Meas. IM-38 (1989) 335.
[6] J.C. Godefroy, C. Gageant, D. Francis, M. Portat, J. Vac. Sci. Technol. A 5 (1987) 2917.
[7] D. Bendersky, J. Mech. Eng. 75 (2) (1955) 117.
[8] K.G. Kreider, Sensors Actuat. A 34 (1992) 95.
[9] G. Wachutka, R. Lenggenhager, D. Moser, H. Baltes, Tech. Digest, 6th International Conference on Solid-State Sensors and Actuators, (Transducers '91), San Francisco, CA, 1991, p. 22.
[10] D. Burgess, M. Yust, K.G. Kreider, Sensors Actuat. A 24 (1990) 155.
[11] H.D. Bhatt, G.C. Fralick, submitted.
[12] H. Baltes, Tech. Digest, 10th Sensor Symposium, Japan, 1991, p. 17.
[13] C.H. Ho, S. Prakash, C.V. Deshpande, H.J. Doer, R.F. Bunshah, Surf. Coatings Technol. 39/40 (1989) 79.
[14] K.G. Kreider, International Conference on Thin Film Thermocouple Research at NIST, ISA/91, 1991, Anaheim
[15] R. Hollanda, Temperature: Its Measurement and Control in Science and Industry, Vol. 1, 64 American Institute of Physics 1 (1992) 1645.
[16] K.G. Kreider, J. Vac. Sci. Technol. A 11 (4) (1993) 1401.
[17] K.G. Kreider, Thin Solid Films 176 (1989) 73.
[18] K.G. Kreider, Mater. Res. Soc. Symp. Proc. Vol. 322, 1994.
[19] K.G. Kreider, Mater. Res. Soc. Symp. Proc. Vol 234, 1991.
[20] R. Vedula, H.D. Bhatt, S.B. Desu, Thin Solid Films, submitted.
[21] E.K Storms, The Refractory Carbides, Academic Press, New York, 1967 p. 1.
[22] Y. Shao, J. Paul, Thin Solid Films 238 (1994) 8.
[23] A.K. Dua, V.C. George, Thin Solid Films 247 (1994) 34.
[24] L.E. Toth, Transition Metal Carbides and Nitrides, Academic Press, New York, 1971.
[25] H.D. Bhatt,R. Vedula, C.T.A. Suchicital, S.B. Desu, Rev. Sci. Instrum., submitted.
[26] L.I. Maissel, R. Glang (Eds.), Handbook of Thin Films, IBM Corp., McGraw-Hill.
[27] R. Steinitz, R. Resnick, J. Appl. Phys. 37 (9) (1966) 3463.
[28] O.A. Golikova, E.O. Dzhafarov, A.I. Avgustinik, G.M. Klimeshin, Heat Transfer-Soviet Res. 5 (2) (1973) 11.